Appl Phys A (2009) 96: 171–188
DOI 10.1007/s00339-008-4981-5

Applied Physics A
Materials Science & Processing

INVITED PAPER

Bulk solar grade silicon: how chemistry and physics play to get a benevolent microstructured material

S. Pizzini

Received: 25 March 2008 / Accepted: 4 November 2008 / Published online: 7 January 2009
© Springer-Verlag 2009

Abstract The availability of low-cost alternatives to electronic grade silicon has been and still is the condition for the extensive use of photovoltaics as an efficient sun harvesting system. The first step towards this objective was positively carried out in the 1980s and resulted in the reduction in cost and energy of the growth process using as feedstock electronic grade scraps and a variety of solidification procedures, all of which deliver a multi-crystalline material of high photovoltaic quality.

The second step was an intense R&D activity aiming at defining and developing at lab scale a new variety of silicon, called "solar grade" silicon, which should fulfil the requirement of both cost effectiveness and high conversion efficiency.

The third step involved and still involves the development of cost-effective technologies for the manufacture of solar grade silicon, in alternative to the classical Siemens route, which relays, as is well-known, to the pyrolitic decomposition of high-purity trichlorosilane and which is, also in its more advanced versions, extremely energy intensive.

Aim of this paper is to give the author's viewpoint about some open questions concerning bulk solar silicon for PV applications and about challenges and chances of novel feedstocks of direct metallurgical origin.

PACS 61.72.-y · 71.55.Cn · 71.20.Mq · 71.55.-i · 81.40.Rs · 84.60.Jt · 81.10.-h

S. Pizzini (✉)
Department of Materials Science, University of Milano-Bicocca, Via Cozzi, 53 Milan, Italy
e-mail: pizzini@nedsilicon.com

S. Pizzini
Nedsilicon SpA, Via Th. Edison 6, Osimo, Ancona, Italy

1 Introduction

In the late 1970s, silicon consolidated its key position in the field of terrestrial solar cells leaving to GaAs the primate for space and concentrators applications.

The situation did not change significantly in the last two decades. In fact, silicon continues to reign supreme in microelectronic applications [1] and covers at the moment, as single-crystal, poly-crystalline (wafers, ribbon and thin films) and amorphous material, more than 90% of the photovoltaic (PV) production, see Fig. 1. Furthermore, almost 80% of more than 1200 MW of the PV modules sold today worldwide is made of crystalline silicon.

As it is well-known, the feedstock used so far to manufacture bulk crystalline silicon for PV applications consists mainly of scraps[1] of electronic grade (EG) silicon produced by a conventional Siemens C process and the Czochralski type of growth.

The limited availability of this kind of feedstock was already in the past considered as a very critical drawback and is today a barrier for the PV market development (which raised in the last years at a rate of 30%/year see Fig. 2) as the demand already exceeds the availability with an unavoidable increase of the purchasing costs of all kinds of silicon available, including hyper-pure poly-crystalline.

Starting from 2005 a significant amount of EG polycrystal supported the PV demand and it is expected that about 60.000 tons of novel PV silicon feedstocks will be needed in the year 2010 to fulfil this material need against a forecasted production of 30.000 tons (see Fig. 3).

[1] As scraps we intend all kinds of silicon not usable for EG applications, like bottoms and heads of ingots, bottoms of CZ crucibles, broken wafers, etc.

It is difficult today to estimate the real evolution of the silicon world production capacity after the year 2010, because most of the estimates foresee impracticable cost and time conditions. We could, nevertheless, predict that the silicon production will possibly grow over 100.000 tons/year in the next few years to come.

It should be, however, noted that in spite of this accelerated growth of the PV market, PV was felt to remain for decades only a marginal solution to the world energy needs, so as far as the forecasted capacity, it would remain a factor of 1000 lower than today's global energy demand.

In addition, the full success of PV in the energy market would require a drastic cost reduction as well as a change of strategy of the electric energy suppliers, which used to think only in terms of multi-GW plants while photovoltaic generation would arise from a myriad of distributed, point-like energy sources, making the grid control a very concerning business.

Today, with a more sensible attention to environmental changes due to CO_2 emissions, the PV scenario looks quite different than before and in the medium to long term the amount of silicon feedstocks needed to satisfy the demand will probably differ by orders of magnitude from the figures previously given.

There is therefore an urgent need to address new R&D efforts dedicated to the industrial development of low-cost processes for the production of a kind of "solar grade" silicon feedstocks, in addition to those aimed at the industrialization of processes for the direct growth of sheets, ribbons and thin films capable to drastically reduce the amount of silicon needed to manufacture high-efficiency solar cells and to drastically reduce or eliminate the amount of silicon lost by ingot slicing processes [2].

The aim of this paper is to present and discuss some physico-chemical problems involved in the development of solar grade feedstocks to be used for bulk silicon multicrystalline solar cells, which will remain the key PV com-

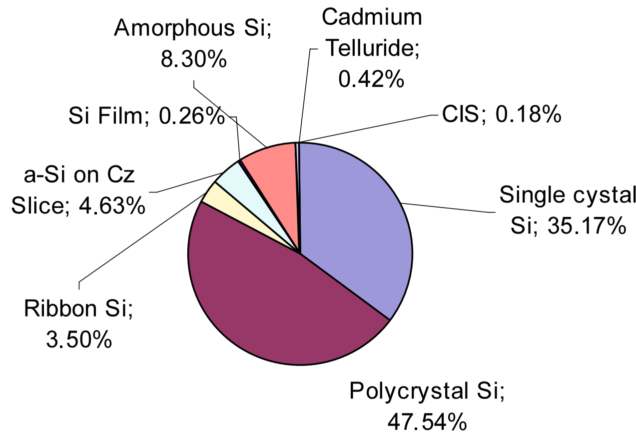

Fig. 1 Distribution of different semiconductors in the PV chain

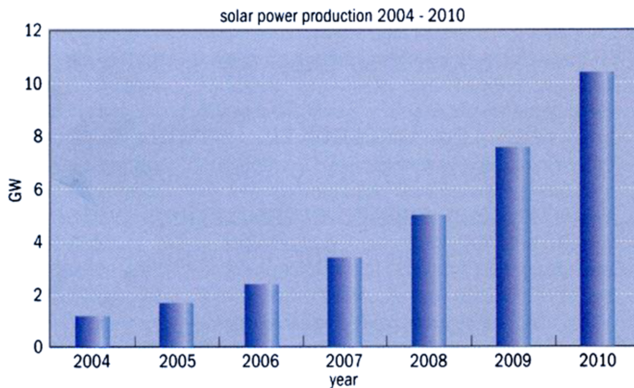

Fig. 2 Past and future growth of the solar PV production (source EPIA)

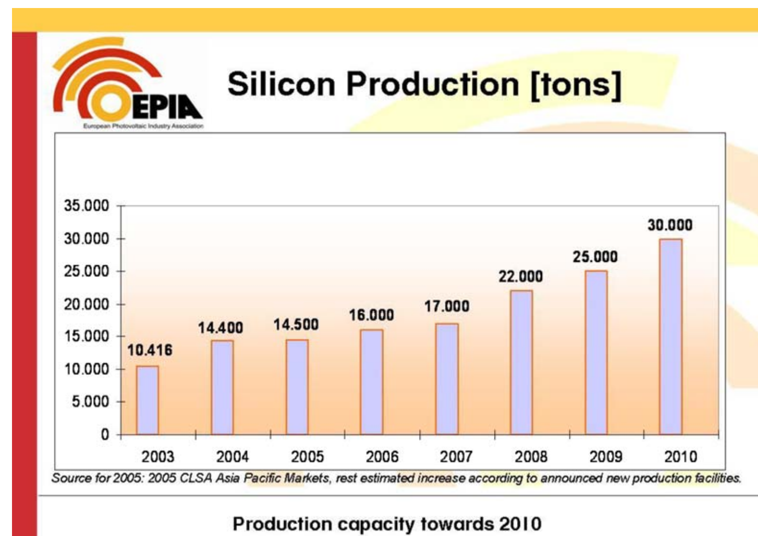

Fig. 3 Poly-silicon production capacity towards the year 2010

ponents for decades or at least until thin-film solar cells will achieve comparable efficiencies, long-term stability and areal costs, and the so-called third generation solar cells will be available.

It will be shown that in solar silicon feedstocks a major role is played by chemical interactions between impurities and structural defects and that, therefore, chemistry should be used to manage the problems associated with defective and impure semiconductors for PV applications.

2 Solar grade silicon as a definition

2.1 Single-crystal material

In the oldest acceptation, solar grade or PV-silicon differs from EG silicon exclusively in terms of its potentially larger metallic impurity content, under the hypothesis that these impurities are better tolerated in PV devices and that the cost of a silicon material is inversely proportional to its metallic impurity content.

The first hypothesis needs to be, of course, demonstrated to be true, as the deep-level impurity content in silicon dictates its capability to work not only as substrate for microelectronic devices but also as an efficient solar energy converter, and it is not so obvious why impurities should be more tolerated in PV silicon.

The hypothesis that the cost of solar silicon should, at least in part, depend on its impurity content is, instead, empirically well-based on the concept that any impurity removing step from an impure intermediate will induce additional energy, investments and labour costs. Therefore, the problem of defining the maximum amount of impurities tolerated for a given efficiency and then with the problem of removal the proper excess of impurity content is crucial at every effect. It is, however, noteworthy that with PV devices conventional intrinsic gettering procedures (which are used to remove impurities introduced during the device processing) could not be adopted as the entire volume of the silicon substrate is active with respect to the absorption of solar photons and to the associated photo-generation of carriers. Therefore, in addition to any preliminary process used to remove impurities from a "dirty" feedstock, only external gettering procedures might be adopted as the final step of any impurity removal process.

The effective impact of the different impurities on the lifetime or diffusion length, and thus on the conversion efficiency of single-crystal silicon solar cells, was one of the problems which were examined at the Westinghouse Research and Development Centre [3, 4] several years ago. To this scope, standard single-crystalline samples containing single or multiple impurities were prepared from Czochralski (Cz)-grown ingots suitably doped and then sliced to wafers, on which chemical analyses and electrical measurements were carried out. Details are reported in [3, 4].

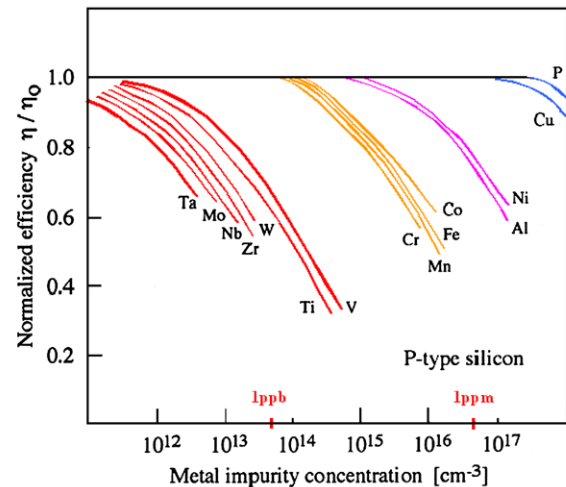

Fig. 4 Effect of the metallic impurity content in single-crystal silicon on the normalized efficiency of solar cells (data from J.R. Davis, R.H. Hopkins, A. Rohatgi [3])

Figure 4 reports a summary of their results, in a η/η° vs. impurity concentration plot, where η/η° is the normalized efficiency of a solar cell and η° is the efficiency of a test solar cell fabricated with single-crystal EG silicon. It could be seen that the majority of the impurities of the first period of transition metals are tolerated at sub-ppma levels, with an exception of Ti, while those belonging to the second and the third periods should be present at sub-ppba levels, instead. This conclusion does not show that single-crystal solar cells have a greater tolerance for impurities than microelectronic devices, where the tolerated amount of impurities is at sub-ppma level, but that, in general, the tolerance limits for impurities of PV-grade silicon depend on the specific impurities

One could, however, afford a preliminary definition of "solar grade" single-crystal silicon on the assumption that the tolerated amount of *a specific impurity* should lie below or very close to the threshold at which the normalized efficiency of a solar cell η/η° deviates from one.

A definition of solar silicon, however, could not, at least, ignore that multiple impurity contamination might change this simple scheme and that many metallic impurities form stable complexes with B and other metallic and non-metallic impurities [5]. Therefore, at least the dopant level should be properly arranged in order to account for the dopant–impurity interaction.

In high-quality single-crystal Si, where dopant–impurity interactions might be neglected, the optimal base B-doping for high-efficiency cells is 0.2–0.3 Ω cm (around 2 ppma) [6].

2.2 Bulk growth of multi-crystalline (mc) solar silicon ingots

It is well-known that two main processes are used for the growth of bulk single-crystal silicon ingots for the electronic market, the Czochralski (CZ) and the Float Zone (FZ) one. Both could be used for the production of wafers for PV applications, getting the best efficiency possible, but both, especially the FZ, were considered so far too expensive for commercial photovoltaics.

Taking into account that an increasing amounts of polycrystalline material will be available in the near future, the use of squared thin wafers of Cz silicon for high-efficiency PV applications might anyway begin to be convenient in the years to come [7]. Large grained and columnar polycrystalline silicon, conventionally named multi-crystalline (mc) silicon is, however, still a relatively low-cost alternative to the Cz silicon and will remain essential when using solar silicon as feedstock. In this material the metallic impurity content is generally low, the oxygen and carbon content is variable depending on the ingot position, and grain boundaries (GB) are generally associated with a variable density of dislocations.

Multi-crystalline silicon is generally prepared with variants of the directional solidification (DS) technique, whose basic features are the high throughput and the relaxed energy consumption costs (<10 kWh/kg vs. 60 kWh/kg for the CZ process).

Its extensive application became possible with the discovery that graphite crucibles, originally used by Wacker Heliotronic for its casting process [8], could be substituted by a quartz crucible lined with silicon nitride, where this lining prevents the wetting of quartz walls by liquid silicon and the consequent destructive tension at the quartz–silicon interface after solidification [9]. In addition, it prevents the ubiquitous heterogeneous nucleation at the graphite walls, typical of the former Heliotronic process as well as the carbon contamination of the ingot with an associated danger of a possible segregation of Sic, a powerful source of minority carrier losses, when the melt is supersaturated.

In their most recent developments, commercial furnaces are designed to grow in a single run, lasting about 50 h, up to 450 kg of silicon to square section ingots at a growth rate around 6 cm/h, leading to a direct growth cost (including electrical energy consumption and crucible cost) close to 10 €/kg. Still under precompetitive conditions, a DS process capable to grow a 450 kg in weight single-crystal ingot is under advanced testing [10].

The use of quartz crucibles could be thought of as the ultimate drawback of the technique, as it will probably limit the achievable size of the ingots, although the today's perspective is to reach one ton capacity for a single batch using superjumbo crucibles and dramatically short growth cycle times.

With an optimized DS process, the liquid solidifies with an almost planar interface and the metallic impurities, thanks to the very low values of their segregation coefficients, are efficiently driven to the very top of the ingot where they concentrate and can be removed at the end of the solidification by sawing the ingot's top.

One of the major problems still occurring today is the loss of a significant fraction of the ingot at the crucible–silicon interface due to impurities released by the silicon nitride coating. On the base of the today's practice, the average quality of the mc-Si is significantly improved with the use of jumbo crucibles.

Crucible-less techniques were also developed and tested in a view of continuous casting process of bulk silicon, but no one went to complete commercialization until now.

It is remarkable that DS growth is less sensible to impurities than CZ, although in both cases the epitaxial growth might degenerate in the presence of massive concentration of impurities accumulated at the liquid–solid interface. While in the case of Cz growth, any significant contamination of the solid–liquid interface by impurity segregation leads to the interruption of the single-crystal growth, massive accumulation of impurities at the solid–liquid interface might cause dendritic growth in the case of DS growth with a total loss of PV properties.

2.3 Properties of multi-crystalline silicon grown from clean feedstocks

Grain boundaries and their properties It is well-known that the properties of multi-crystalline silicon are the *local* properties, as they depend on the bulk properties of each single grain and on the (structural and electrical) properties of each single GB and on its contamination. It is also well-known from the literature that a single grain might be contaminated by dissolved metallic and non-metallic impurities and might be severely affected by extended defects, such as dislocations and twins. In turn, the structural properties of GBs, which might be depicted as true internal surfaces, are affected by the specific reciprocal mis-orientation of the neighbouring grains. Their physico-chemical properties are ruled by the residual unsaturated (dangling) bonds, by the impurities segregated on them and by other structural defects (dislocations and precipitates). Highly symmetric impurity-free GBs might be entirely reconstructed and therefore are electrically inactive, while low-symmetry GBs are only partially reconstructed and present both chemical and electrical activity. In the first case, we expect only the presence of shallow states associated to dilated or distorted bonds, in the second one, deep gap states associated to unsaturated bonds.

Thermodynamics and chemistry are responsible for GB reconstruction during growth or any subsequent high-temperature treatment, and also during the solar cell fabrication

processes. The extent of thermodynamically possible reconstruction is given by the minimization of the excess Gibbs free energy due to presence of defects. Reconstruction in *clean* materials would imply only structural reconstruction. In the presence of impurities a kind of chemical reconstruction might play a major role based on impurity interaction with GBs, which also act as heterogeneous nucleation centres for precipitation of supersaturated impurities. Chemical interaction with metallic impurities leads, even at moderate temperatures (300°C), to silicide bond formation [11] while interaction with non-metallic impurities (O, C, N) leads to more complex bond structures including oxide, silicate, carbide and nitride bonds. Depending on the bond formation energy deep gap centres associated with unsaturated bonds might be removed from the gap and transformed in electrically inactive centres. These kinds of processes, of which the best-known involves hydrogen, lead to the unsaturated bond passivation and, possibly, to GB inactivation.

As a consequence of impurity segregation at GBs, the formation of an impurity denuded zone occurs, whose depth depends on the diffusivity of the specific impurity and might be approximated by its diffusion length $L_D = \sqrt{Dt}$, where D is the diffusion coefficient and t is the time. This approximation holds uniquely if one can neglect the presence of GB strain fields, which play an additional role in the collection of the impurities.

Outside the denuded region, the intra-grain properties should be quite inhomogeneous and one might assume that they are dominated by the slow-diffusing impurities, like carbon, oxygen and nitrogen, and, possibly, by crystal defects. Fast diffusing impurities, like the metallic ones, easily segregate at GBs and their depletion region might extend through the entire volume of the grain.

The presence of intra-grain defects has been recently demonstrated by Jigging Lu et al. [12] in nitrogen-rich silicon poly-crystalline sheets. They showed that silicon oxynitrides do precipitate preferentially at GB, leaving a well-defined denuded zone and that the intra-grain defects consist of stacking faults, associated to homogeneously nucleated oxide precipitates.

Intra-grain defects consisting of α silicon nitride and iron silicide have been also observed close to the external surface of mc-Si ingots grown in quartz crucibles coated with silicon nitride [13].

Impurity segregation at extended defects has been recently modelled [14] in relationship to silicon microelectronic processes, but their features were also systematically studied in relationship to multi-crystalline materials [15], in view of the development of specific extrinsic gettering processes[2] [16].

We would like to briefly mention here the key role played by point defects and by stress fields on the precipitation of supersaturated impurities at GBs. For an example, it was shown that, in the case of oxygen and carbon contaminated samples, oxygen segregates in close correspondence with the geometrical position of the GB while carbon presents two satellite peaks spatially separated from the oxygen peak [17]. This result might be understood by assuming that the compressive strain field generated by SiO_x segregation at the GB is compensated by the tensile field caused by C agglomeration or segregation leading to local conditions of mechanical (hydrostatic) equilibrium, in good agreement with the well-known exigent volume models of Tice and Tan [18], and Hub [19] which accounts the different molar volumes of Si, SiC and SiO_2, being $V_{SiO_2} \approx 2V_{Si}$; $V_{SiC} \approx \frac{1}{2}V_{Si}$. In carbon-free samples, instead, the strain field associated with oxygen segregation is released by dislocation emission. The dislocations are punched out by the precipitates when self-interstitials supersaturation conditions occur [20]. Silicon self-interstitials (Si_i) are, in fact, reaction partners in the oxide phase formation, which can be formally written as

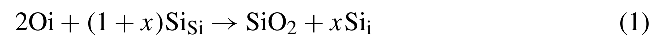

$$2\mathrm{Oi} + (1+x)\mathrm{Si_{Si}} \rightarrow \mathrm{SiO_2} + x\mathrm{Si_i} \quad (1)$$

The emission of the Si interstitials produces locally the volume needed to accommodate the oxide phases in the silicon matrix. Self-interstitials are, as well, the reaction partners in the SiC formation

$$2\mathrm{C_i} + \mathrm{Si_{Si}} + \mathrm{Si_i} \rightarrow 2\mathrm{SiC} \quad (2)$$

As in solid state reactions or transformations full equilibrium conditions are satisfied only in the simultaneous presence of thermodynamic and mechanical equilibrium, of which the last implies the absence of local stresses, we might foresee the achievement of full equilibrium conditions when O and C co-segregate as spatially separate phases.

In addition, as could be inferred from simple thermodynamic considerations, every internal surface might behave as a phase of reduced dimensionality with properties substantially different from the bulk phase due to the different coordination and bonding. Grain boundaries should present such behaviour and the impurity segregation at GB might be discussed as an impurity repartition between phases of unlike dimensionality, in the same way one discusses the equilibrium between condensed phases of different composition [21].

The physico-chemical properties of a poly-multi/crystalline material depend, therefore, in a very complex manner

[2] We use here the term "gettering" or "segregation" for any process which involves the equilibrium repartition of an impurity between a bulk phase and an interface. In the IC technology gettering is a process-induced segregation at ad hoc created surfaces or in depth regions where unwanted impurities are deliberately collected and inactivated.

on the properties of both the GBs and the bulk of the grains and are therefore, as said before, true *local* properties, as different equilibrium conditions arise in correspondence of specific grains or specific GBs.

They will depend mostly on their intra-grain properties in the case of diluted solutions of impurities. Here, segregation of impurities at GB induces impurity depletion within the grain volume and bond formation at unsaturated bonds and, then, possibly, GB passivation.

When supersaturation conditions occur, extended defects behave as heterogeneous nucleation centres for the second phase formation: in this case the GB properties are influenced by the electronic properties of the deposited phases, which, in turn, might be the nucleation centres of dislocations if in their presence a stress/strain field sets-up.

Quite generally, therefore, one has to conclude that the properties of multi-crystalline silicon are dominated by impurities, GBs and dislocations.

Even in the case of extremely pure materials, however, GBs and dislocations must be, for thermodynamic constraints, always contaminated by residual impurities. We will show in the next section that this happens for GB contaminated with oxygen, but the same evidence has been given for dislocations, whose electrical activity was demonstrated to depend on gettered impurities [22].

The discussion of the electrical activity of GBs requires, therefore, a deep insight on the chemical contamination of the boundary, as will be shown in the next sections.

Effect of grain boundaries on the electronic properties of mc-Si The ubiquitous presence of grain boundaries (GB) and dislocations in poly-crystalline silicon, independently of the preparation processes, was for years felt an insurmountable limit for its use in photovoltaics, as GBs and dislocations are known to behave as killers of the minority carrier lifetime.

It is, in fact, widely accepted that GBs introduce deep levels in the gap acting as recombination centres of minority carriers. These deep levels are attributed to intrinsic structural defects, such as dangling bonds, dislocations or extrinsic impurity contamination.

For an example, Seifert et al. [23] reported that the recombination activity of GBs is related to the density of dislocations in/at the boundary and that impurity segregation produces an additional activity.

As a further example, Chen et al. [24, 25] have studied the effect of GB character (Σ values) and boundary plane on the electrical properties of GBs. They have demonstrated that the recombination activity at room temperature of contamination-free GBs is weak and the GB structure has minor effect on the electrical GBs properties. They have also studied the impact of the impurity contamination on the recombination activity of grain boundaries in mc-silicon cut from different solidification positions of a B-doped ingot [26, 27]. The metallic impurities content in the samples studied, except for Fe, was below the detection limit. The Fe concentration was below 5×10^{12} cm^{-3} at the central position and was of the order of 10^{15} cm^{-3} at the top and bottom positions. It was shown that in the central and top (solidified last) sections of the mc-Si ingot, the recombination activity of GBs was weak at 300 K, whereas in the bottom (solidified first) section some GBs showed enhanced recombination activity, which was attributed to the effects of iron and additional impurity contamination.

From the very large amount of papers which have been dedicated to the study of the electrical properties of grain boundaries (GBs) and dislocations in semiconductor materials [28–32] it comes out, however, that in large grained, columnar and impurity-free mc-Si the GBs become often a tolerable structural defect.

In addition, as GBs getter metallic and non-metallic impurities, the properties of mc-Si might be comparable, within the grains, to that of single-crystal silicon even in the presence of substantial impurity content. Large columnar grains should minimize, therefore, carrier recombination and mobility losses at GBs, provided their orientation is parallel to the drift and diffusion paths of carriers to the junction and the base contact.

It is well-known, in fact, that in mc-Si ingots grown from feedstocks of EG origin there is no significant influence of GBs on the diffusion length for L_{GB} values larger than 10–30 cm^{-1}, where L_{GB} is the length of GBs in a square cm. With these L_{GB} figures, the average size of a crystallite is between $0{,}5 \times 0{,}5$ cm and $0{,}25 \times 0{,}25$ cm.

Furthermore, already in the 1980s [33] it was shown that the average values of the diffusion length in large grained directionally solidified (DS) silicon prepared with EG feedstocks were close to those of Cz silicon, reaching values often larger than 200 μm.

The primary cause of a lower conversion efficiency of solar cells based on mc-Si, when compared to that of single-crystal cells, was shown to be, instead, due to the presence of regions of high minority carrier recombination generally characterized by a high dislocation density [34–36].

It was therefore concluded that any improvement in the PV behaviour of large grained poly-crystalline materials passes through the improvement of the intra-grain properties (impurity content, dislocation density, precipitates), also assuming that the impurity effect might be severe in the case of low-grade feedstocks, as it will be shown in this and in the next sections.

Concerning the dislocation density and their recombination activity, it could be shown that they are not independent variables of the system.

In fact, the dislocation density might depend on the concentration of specific impurities (as will be shown in the next

section) and their electrical activity depends on impurities, because even traces of dissolved impurities might segregate on them, changing their recombination activity. We mention again here that while *clean* dislocations should be electrically inactive at room temperature because of structural reconstruction [37, 38] their decoration with transition metals would introduce deep levels [39].

Dopant impurities and their interaction with extended defects The knowledge of the threshold concentration of B (and P) as single or multiple impurities is of primary importance for the design/procurement of future solar grade feedstocks, as it is well-known from the literature [40] that at even at dopant concentrations lower than 10^{18} cm^{-3} these shallow acceptor traps affect substantially the carrier lifetime.

Unfortunately enough, they represent, together with carbon, the least easily removable impurities from a highly doped silicon feedstock or from a commercial metallurgical (MG) silicon source, where, based on the average content of boron in the quartz used in the MG silicon industry, a B concentration greater than 10^{18} cm^{-3} (20 ppma) is the expected figure. This concentration would lead to a bulk resistivity value around 4×10^{-2} Ω cm, and then to the usefulness of this material for PV applications, even in the absence of metallic impurity concentration.

Using solidification techniques boron removal is impossible, as its segregation coefficient is close to one: therefore liquid–liquid extraction techniques using, for example, oxidic slags [41] or metals as well as gas sparing techniques with wet argon should be employed [42] with rather complicated and cost-intensive technological procedures as will be seen in the last section of this paper.

One possible solution of the problem could be the electrical compensation of boron with donors, like P or as, but the amount of possible compensation is still an unknown. Our studies [43] showed that the lifetime and the PV properties of p-type single-crystal silicon are not appreciably affected by the contemporaneous presence of donors and acceptors; provided the *excess* acceptor concentration is lower than 5×10^{16} at cm^{-3}. Above this threshold, the lifetime decreases and the relative normalized cell efficiency drops suddently from values close to 1 to values close to 0.5. Apparently, the density of the electrostatically bonded B–P pairs does not influence the minority properties, while the excess acceptor concentration dominates the same properties. In the presence of extended defects, as is the case of mc-Si, it could be expected that extended defect–impurity interaction would play a complex role on the ultimate efficiency of solar cells, due to the fact that extended defects induce deep levels in the gap and behave simultaneously as deep sinks for metallic (and non-metallic) impurities via chemical bond formation and stress field relief.

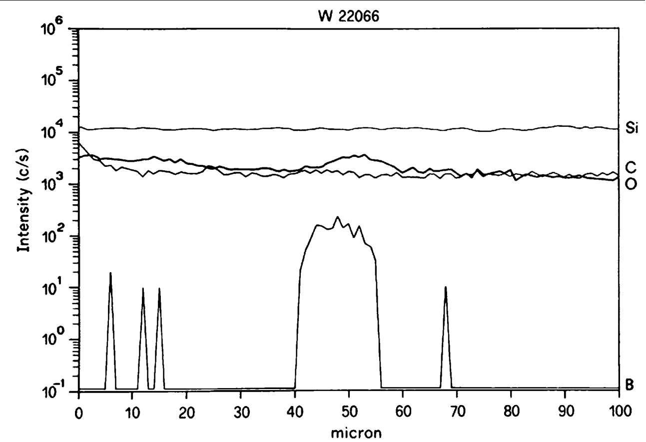

Fig. 5 Boron segregation at GBs in carbon-rich mc-Si [47]

Recent results reported by Geerligs et al. [44] show, however, that the effect of strong compensation would be noticeable, but not very important, considering that the capture cross-section of neutral dopants should be of the order of 10^{-17} cm^2.

If dopants segregate at extended defects, they should leave partially or totally depleted the bulk of the grains. As a result, dopant deactivation might occur or a change of the recombination activity of extended defects. In good agreement with this hypothesis it is known that the optimal base boron doping takes an empirically determined value between 1 and 3 Ω cm (≈0.15 ppma) for PV-grade silicon [6], which is one order of magnitude larger than for CZ silicon. The difference is accounted for on the assumption that dopant deactivation might occur, in a good agreement with many recent papers which demonstrate that boron segregation occurs at specific silicon surfaces.

As an example it has been shown [45] that extraordinary boron segregation occurs at Si(111) surfaces in a planar doping process. It has been also demonstrated [46] that the segregation ratio $r_\mathrm{d} = I_\mathrm{s}/I_\mathrm{b}$ of boron at Si(111) surfaces, where I_s is the boron concentration at the surface and I_b is the boron concentration in the bulk, remains close to 1 at low temperatures (400–570°C), increases to 5.5 in the 570–720°C range and jumps to 42 at 720–750°C. At even higher temperatures r_d decreases systematically and reaches a value of 25 at 900°C. This means that only a fraction of B is electrically active as a consequence of segregation.

Eventually, the segregation of B at GBs as B–O complexes was demonstrated by SIMS measurements (see Fig. 5), in the presence of a significant amount of carbon [47]. This event is signalled by a hundredfold increase of the B signal with respect to the boron background of the sample and by a simultaneous increase of O-content at GB and could be interpreted as a good example of a segregation dominated by a chemical reaction.

Additional measurements were also carried out on Al-doped multi-crystalline samples [48], as Al is an acceptor

impurity which could be present in large amounts in MG feedstocks and which presents, like other dopant impurities, unfavourable segregation coefficients. It was shown that the hole mobility and the carrier concentration decreases for Al concentrations greater than 10^{17} cm^{-3}, while the diffusion length decreases monotonically already for Al contents greater than 10^{16} cm^{-3}. Eventually, it was suggested [49] that part of the Al segregates at GB with their consequent passivation and those microprecipitates are observed by TEM measurements in heavily concentrated ($>10^{19}$ cm^{-3}) samples. The presence of two deep levels at 0.315 and 0.378 eV was finally detected by means of deep-level transient spectroscopy (DLTS), of which the first is a recombination centre and the second is a whole trap. Both are possibly associated with the Al–O centres detected by Marchand and Sha in single-crystal silicon [50].

2.4 Native impurities (oxygen, carbon, nitrogen) in mc-Si and their interactions

The key role of oxygen and carbon, whose concentration depends on the growth conditions, on the electrical activity of GBs was already observed in our earliest experiments and later one by Radzimski et al. [37].

We have experimentally demonstrated at first that the concentration of dissolved oxygen N_O and carbon N_C in DS silicon is a quasi-equilibrium property, defined by the constant

$$K = N_O \times N_C \tag{3}$$

which also accounts for the repartition coefficient of carbon and oxygen within the solid and liquid phases [50].

In our experiments with small (few Kg in weight) mc-Si ingots, using feedstocks of EG origin, their concentration varied continuously from the bottom to the top of the ingot, with values which ranged from 10 ppma O and 2,5 ppma C to 2,5 ppma O and 10 ppma of C.

This range of concentrations is also typical of commercial ingots nowadays, as it is shown in Fig. 6.

These studies allowed the identification of a region where second-phase formation occurs with the precipitation of an (oxi)-carbide phase. Precipitation, as monitored by microstructural examinations, occurs when the carbon concentration is greater than 7 ppma and the oxygen concentration is lower than 2.5 ppma. As the oxygen content takes these critical values only in correspondence of the least fraction solidified (see again Fig. 6), precipitates are confined on the top of the ingot.

We have also shown that the diffusion length of the minority carriers depends on the oxygen and carbon content and takes the largest values in correspondence with solutions containing equivalent concentrations of oxygen and carbon. This result might suggest that in this case the segregation

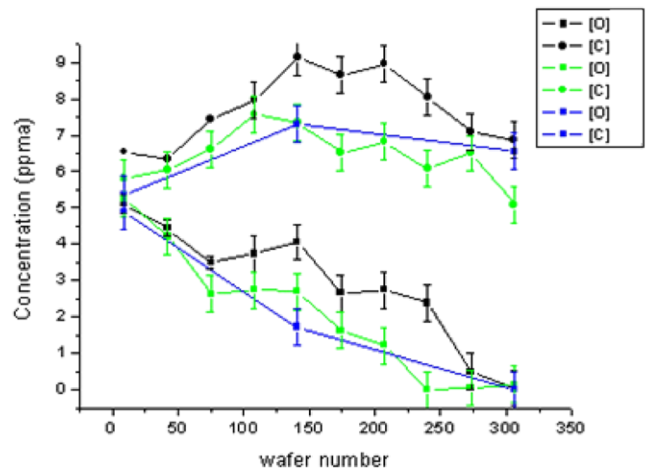

Fig. 6 FTIR oxygen and carbon concentration profiles in an n-type multi-crystalline silicon ingot (the *bottom* region starts *on the left*): the measurements were carried out in different positions of the same wafer

process would involve the simultaneous precipitation of silicon oxide and silicon carbide, thus allowing the achievement of local conditions of mechanical equilibrium due to a compensation of tensile and compressive fields associated with the segregation of these compounds (see reactions 1 and 2 and comments therein).

These results show that a correlation exists between strain compensation and co-segregation of oxygen and carbon. It has been, in fact, proven that the dislocation density in as-grown, *clean* multi-crystalline silicon [36] is not an independent variable of the system, as it decreases with the increase of the oxygen content and increases with the increase of the carbon content. As the diffusion length of minority carriers depends only slightly on bulk oxygen and carbon content, this result shows that interaction of oxygen and carbon with GBs and, possibly, with dislocations occurs and that the decrease of diffusion length with the increase of both O and C depends on an increase of the recombination activity of extended defects.

As the dislocation density decreases with the increase of oxygen while it increases with the increase of carbon, one could infer that the increase of recombination activity in multi-crystalline silicon is associated, in oxygen-rich materials, to O-segregation at GBs and to the increase of dislocation density in carbon-rich silicon.

The actual localization of oxygen and carbon segregation (infra-grain or at GB) was investigated using FTIR [51] and SIMS [52] measurements in scanning or mapping configuration.

It is interesting to remark that the IR-active interstitial oxygen absorbance at 1107 cm^{-1} does not change significantly when the light spot was scanned from the bulk and across a GB in an as-grown and heat-treated sample at 1150°C, although a 10% increase of the absorbance is detected in the heat-treated sample.

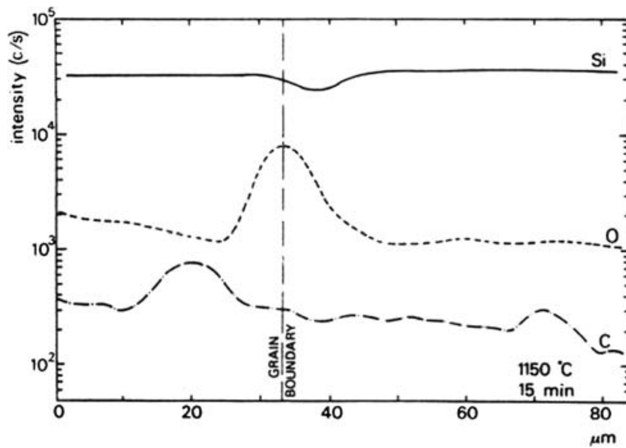

Fig. 7 Segregation of carbon and oxygen at grain boundaries in mc-Si after annealing at 1150°C. The segregation of the oxide at GB is revealed by the decrease of the silicon signal in correspondence with the increase of the oxygen signal [52]

Instead, an excess free carrier absorbance is observed when the light beam is scanned across the GB in both the as-grown and heat-treated sample. It implies that the GBs are decorated by metallic impurities already in the as-grown state, with deep implications on their electronic structure.

The IR absorption at 1107 cm^{-1} is however specific for self-interstitial oxygen and do not monitor the oxygen associated with oxide precipitates, differently from SIMS measurements which detect the total oxygen (and carbon). SIMS measurements [17] allowed to infer that their segregation occurs only in the heat-treated sample, but that only oxygen segregates in close correspondence with the position of the GB while C segregates in correspondence of two satellite peaks, several um far from the geometrical position of the GB, as it is shown in Fig. 7.

The decrease of the Si signal of the GB site indicates that an oxygen rich silicon phase is segregating at the GB.

Thus, it seems it has demonstrated that carbon and oxygen, in heat-annealed samples, preferentially segregate at GB, which apparently behaves as heterogeneous nucleation centre for the sole oxygen precipitation, while carbon nucleates homogeneously.

To reduce or eliminate the consequences of growing silicon from high oxygen or carbon melts, specific defect passivation procedures should be foreseen and adopted, as is the case of EFG ribbons grown in a carbon-rich ambient.

The behaviour of multi-crystalline samples containing a slight excess of oxygen over carbon, carefully studied in function of the annealing temperature [53, 54], did allow a better understanding of the crucial role of oxygen.

It was, in fact, observed that both the local bulk diffusion length and the GB contrast determined by means of electron beam-induced current (EBIC) measurements show a strong decrease after a two-step annealing at 450°C and then at 650°C. In addition, it was shown that the EBIC contrast presents a maximum at 650°C while the diffusion length decreases monotonically with the increase of the annealing temperature in this specific range. These results might be interpreted by considering that oxygen segregated at temperatures higher than 650°C passivates GBs. Instead, the old and new thermal donors, generated at 450 and 650°C, respectively, degrade the diffusion length.

This conclusion is supported by local measurements of electrical activity of GBs, carried out by electrical conductivity measurements, which demonstrated that not only the minority carrier but also the majority carrier properties ones are influenced by impurity contamination.

Trans-barrier DC conductivity measurements carried out on single GBs which were contaminated with carbon, oxygen and oxygen and carbon showed [55], in fact, that only GBs decorated with carbon exhibit a temperature activate behaviour, while GBs decorated with oxygen display a behaviour which is comparable with that of single-crystal silicon.

It could be concluded that the deep traps and gap states responsible of mobility drops and minority carrier recombination losses are associated with the segregation of native impurities and not "intrinsic" to interface states, in good support of our previous considerations about *clean* GB, that are intrinsically thermodynamically unstable objects.

It is quite interesting to consider that similar considerations were recently raised by us for the recombination activity of dislocations in EG silicon [56].

It could be concluded that multi-crystalline silicon in which carbon-oxygen compensation occurs presents close similarities with crucible grown CZ silicon.

Instead, we must foresee serious degradation effects in the quality of silicon prepared along the MG silicon route when its carbon content is not carefully controlled [57].

3 Metallic impurities

An attempt to model the behaviour of mc-Si in the presence of metallic impurities was carried out, among others, by the present author, under the assumption that the lifetime of un-doped and uncontaminated samples might be calculated considering that the recombination events at recombination centres in the bulk of the grain and at extended defects are independent, that impurities segregated at grain boundaries and dislocations are electrically inactive and that oxygen and carbon interact with GBs inducing recombination effects. This model was experimentally tested in the case of mc-Si-doped with Ti, V, Cr, Fe and Zr [58, 59].

The results of this investigation showed that at metallic impurity concentrations lower than 10^{12}–10^{13} cm^{-3} the model assumptions are closely followed by all the examined impurities, while important deviations occur above this

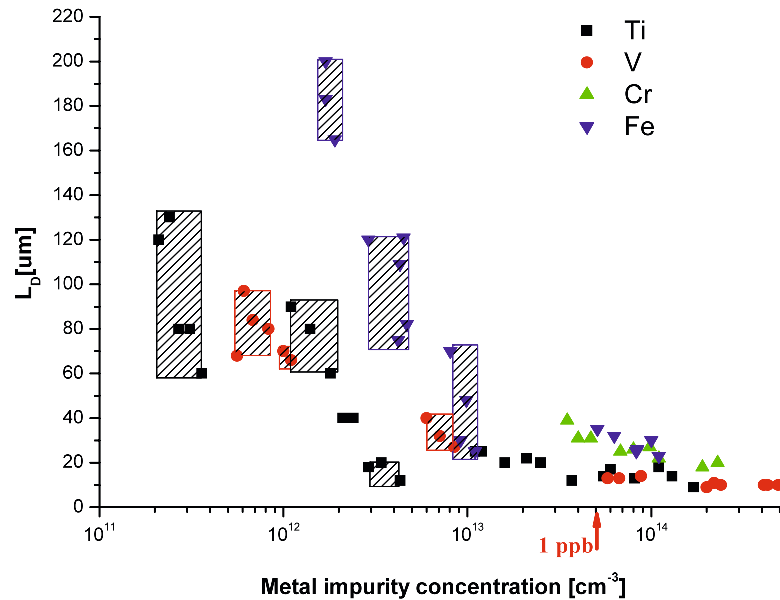

Fig. 8 Influence of the impurity concentration on the diffusion length of mc-Si

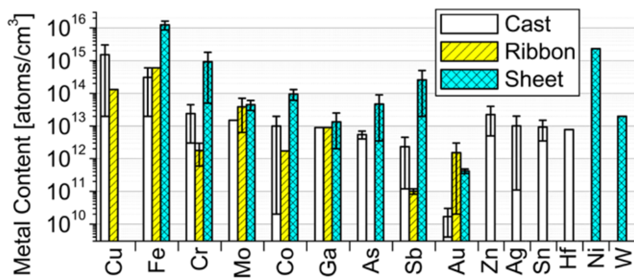

Fig. 9 Metallic impurity content of commercial mc-Si materials (with kind permission of T. Buonassisi)

threshold, indicating that interaction with extended defects occurs, inducing a simultaneous decrease of the diffusion length.

A summary of the results reported in [58] and [59] is displayed in Fig. 8, which shows that for V and Ti a strong decrease of the diffusion length is observed at concentrations greater that 10^{12} cm^{-3} (>0.05 papa). Moreover, it is apparent that iron is the least dangerous impurity, while V and Ti are extremely efficient recombination centres.

As the metallic impurity concentration in commercial cast silicon prepared from EG silicon rejects of generally high purity, ranges around 10^{13} cm^{-3} (0.5 ppba) or less [60–63], see also Fig. 9, one might expect moderate or high values of its diffusion length, in spite of the fact that this value largely exceeds the threshold for EG silicon (about 10^9 cm^{-3}). Actually, in very good agreement with our results reported in Fig. 8, at least for some common contaminants (Fe, Ni and Cu, see Fig. 10) the diffusion length decreases systematically when the impurity content exceeds the EG silicon threshold, showing that metal contamination is a key limiting factor in solar cell performance at any concentration level.

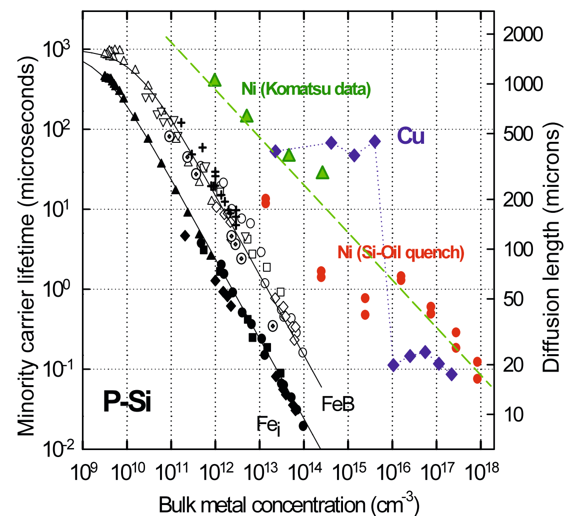

Fig. 10 Effect of Cu, Ni and Fe on the lifetime of p-type silicon [60]

The problem of the impurities in solar-grade silicon has been also considered by Gerligs et al. [64] and by McDonald et al. [65]. Here, according to Gerligs, the estimated impurity level for 3% reduction of cell efficiency are around 0.1 ppma for Al and Ti and around (possibly less) than 10 ppma for C and Fe.

4 Impurity localization in multi-crystalline silicon

4.1 Introductory remarks

The previous considerations about impurity contamination do not take into full account possible interaction effects between impurities and extended defects, which might lead

to a greater or worse tolerance of impurities in the case of mc-Si.

To account for it, we shall start [66] considering that the distribution of impurities, in thermodynamic equilibrium, between two phases, is ruled by their chemical potentials μ_i.

This condition might be written as follows

$$\begin{aligned} &\mu_i(\alpha) = \mu_i(\beta) \\ &\mu_i(\alpha) = \mu_i^\circ(\alpha) + \mathrm{RT}\ln a_i(\alpha) \\ &\mu_i^\circ(\alpha + \mathrm{RT}\ln a_i(\alpha) = \mu_i^\circ(\beta) + \mathrm{RT}\ln a_i(\beta) \\ &\mu_i^\circ(\alpha) + \mathrm{RT}\ln x_i(\alpha)\gamma_i(\alpha) = \mu_i^\circ(\beta) + \mathrm{RT}\ln x_i(\beta)\gamma_i(\beta) \end{aligned} \tag{4}$$

where α and β are the two phases, possibly of unlike dimensionality and i is the impurity. Then, the repartition coefficient $K^{\alpha\beta}$ of the impurity i between the two phases is given by

$$\begin{aligned} K^{\alpha\beta} &= x_i(\beta)/x_i(\alpha) \\ &= \gamma_i(\beta)/\gamma_i(\alpha)\exp -\left[\left(\mu_i^\circ(\beta) - \mu_i^\circ(\alpha)\right)/\mathrm{RT}\right] \end{aligned} \tag{5}$$

and is the complex function of activity coefficients $\gamma_i(\beta)$ and $\gamma_i(\alpha)$, which in turn depend on the concentration, and of the standard chemical potentials μ_i° of the impurity i in the two phases.

The standard chemical potentials $\mu_i^\circ(\beta)$ and $\mu_i^\circ(\alpha)$ are a measure of the energetics of i in the two phases arising from different configurations and bonding character. If the impurity i in the two phases behaves ideally, as is the case of dilute solutions, the ratio $\gamma_i(\beta)/\gamma_i(\alpha)$ equals one or is constant and the segregation coefficient $K^{\alpha\beta}$ is a sole function of the standard chemical potentials of i in the two phases.

The same condition holds for the repartition of an impurity i between a bulk solid phase (b) and an interface (s), where the last could be treated thermodynamically as a phase of reduced dimensionality

$$\begin{aligned} K &= x_i(s)/x_i(b) \\ &= \gamma_i(s)/\gamma_i(b)\exp -\left[\mu_i^\circ(s) - \mu_i^\circ(b)/\mathrm{RT}\right] \end{aligned} \tag{6}$$

Here, the difference $\mu_i^\circ(s) - \mu_i^\circ(b)$ is the excess surface/interface energy.

Therefore, impurities present in a solid phase might segregate spontaneously at any interface, the driving force being the difference in their chemical potentials or activities, until the equilibrium condition is reached when their chemical potential at the interface is equal to that in the bulk phase.

Two different situations might be, however, foreseen, depending on the thermal conditions at which the segregation occurs.

In fact, segregation might occur during the crystal growth process, which includes a constant temperature stage during crystallization, with impurities normally in under-saturated conditions as well as during the cooling-down step, where thermal gradients could set-up and the impurities could reach supersaturation conditions. Here, the segregation yield might depend also on kinetic parameters, as impurities have to diffuse from the bulk to any active interface defect before being captured, with a complex interplay between thermodynamic and kinetic parameters.

Segregation might, however, also occur in thermal equilibrium conditions during each of the annealing stages to which the crystal has to be subjected during the solar cell fabrication process or during each intentional annealing process addressed at impurity gettering or passivation.

These last processes were predicted by V. Kveder et al. [67] and received as well substantial experimental support [68, 69].

In the other cases a preliminary analysis of the local segregation features is the background for a subsequent theoretical modelling.

4.2 Impurity localization in mc-Si: experimental results

Several attempts addressed at monitoring of the segregation of metallic impurities at GBs has been carried out in the years starting from the very early works of Kasmerski et al. [70] and Kasmerski and Russell [71], who using scanning Auger microprobe and SIMS measurements showed that Ni, Al, Ti, Cu and Mg could be detected at fractured GBs at concentrations higher than 10^{18} cm^{-3}, several orders of magnitude larger than the bulk grain concentration which was of the order of 10^{11}–10^{15} cm^{-3}.

As shown before, using SIMS experiments, Pizzini et al. [51] were able to demonstrate that also oxygen and carbon segregate at GBs.

Similar effects of Cu and Ni at GBs, possibly associated to the previous precipitation of oxygen, have been identified by Maurice and Coliex [72] on $\Sigma = 25$ bi-crystals annealed at 900°C using energy dispersive X-ray spectroscopy and EBIC measurements and by Ihlal et al. [73] on Cu- and Ni-contaminated $\Sigma = 25$, $\Sigma = 13$ and $\Sigma = 9$ bi-crystals annealed at 1100°C. These last authors were able to identify, using EBIC measurements, the formation of about 100–150 μm thick denuded zone on both sides of the interface, and the formation of silicides precipitates in the bulk of the grains. Here, the authors tentatively correlate the gettering efficiency of individual GBs to the extension of the denuded zone by modelling the excess interface energy and of the associated strain fields.

Recent work showed also that metals segregate in form of submicron-size precipitates,

The segregation of submicron-size precipitates of Cr, Fe and Ni in mc-Si in regions of high minority carrier recombinations, which could be identified to represent GB regions, was, in fact, detected by S. McHugo et al. using synchrotron

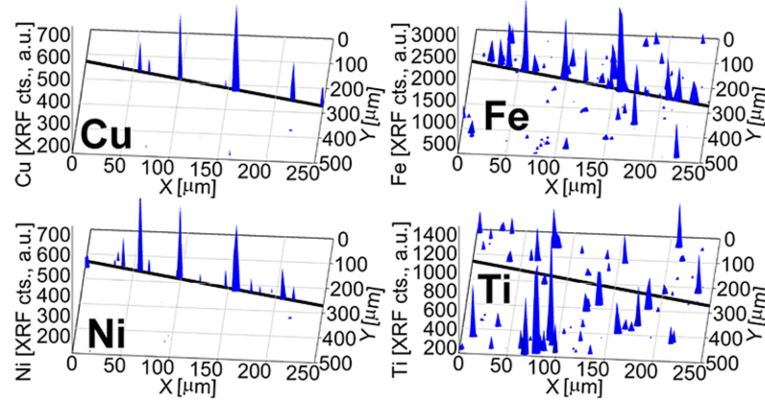

Fig. 11 Segregation of Cu, Ni and Fe and Ti in mc-Si. The difference between Cu and Ni and Fe and Ti is immediate. After Buonassisi [76]

based XR fluorescence [74]. The same authors clarified in a later paper [75] using the near edge structure of XR absorption spectra, that the iron precipitates consist of iron oxides or silicates, which are more stable than the corresponding silicides.

Similar experiments were carried out by Buonassisi et al. [76] for the analysis of copper-rich precipitates in silicon, who showed that copper is an ubiquitous contaminant of silicon and that its segregation features (composition of the phase) depend on the defect structure and on the oxygen content of the silicon matrix.

In addition, they showed also that in as-grown mc-silicon copper-rich clusters were located at GBs, together with nickel, both not intentionally added to the melt from which the ingots were solidified.

Some metal segregation maps are reported in Fig. 11, which shows that Cu and Ni segregate in close correspondence of the GBs, titanium is almost fully dispersed in the matrix, while iron is in an intermediate situation.

It is interesting to note that the plot of the fraction of metal particles segregated off-GB as a function of the product $\Psi = D \times S$ (see Fig. 12), where D is the diffusivity and S the solubility, shows that high Ψ values favours the segregation of particles in correspondence to GBs, as is the case of Cu and Ni, which, in fact, tend to accumulate at a few energetically favourable regions within the device (e.g. high-sigma twins, non-twinning GBs), while Ti and Fe tend to be more dispersed throughout the device. These results are extremely useful for the design of appropriate gettering procedures, addressed at the removal of excess metallic impurity content in solar silicon feedstocks. A conventional external gettering process should be favourable for Fe and Ti removal, while extended defects will compete with surface traps in the case of Cu and Ni. According to Seibt et al. [77] $NiSi_2$ nano-precipitates are efficient recombination centres, which can be passivated in p-type Si, while their activity remains unchanged in n-type silicon.

As already anticipated by the present author for the case of Er-O-dislocation interaction [78] it should also be taken

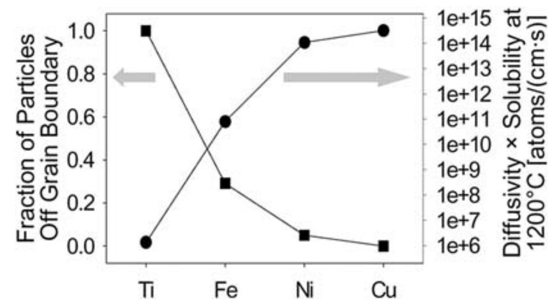

Fig. 12 Off-grain and in-grain segregation of Cu, Ni and Fe and Ti in mc-Si. After Buonassisi [76]

into account that oxygen competes strongly with metals on the interaction with silicon atoms at the interface or at the boundary of an extended defect, depending on the Me–O, Si–Me and Si–O bonding energies. When the Me–O bond formation prevails, extended defects work as heterogeneous nucleation centres, while, when the Si–O interaction prevails, metals might be gettered at extended defects with Me–O bonds.

These results might also be used to explain why extrinsic gettering processes using near surface phosphorous and aluminium deposition are shown to be very effective in the case of silicon microelectronic processes [79] as well as for impurity gettering from EG-dislocated silicon [80], but might work poorly with mc-Si. It can be argued, in fact, that once the metallic impurities interact with extended defects giving origin to stable oxide or silicate bonds, their extraction by gettering processes is a very difficult task.

5 Processes potentially interesting for the procurement of solar silicon feedstocks

Two main streams are considered now of potential interest for solar grade feedstocks.

The first still relies on the use of gaseous precursors of silicon, i.e. of silane and chlorosilanes, the second on metallurgical silicon.

5.1 Gas phase processes

The most important gas phase process, characterized by an extremely high rejection rate for boron, is still the Siemens C process, which, as it is well-known, is based on the high-temperature reduction of purified trichlorosilane ($SiHCl_3$ or TCS) with hydrogen to poly-crystalline silicon in vertical batch reactors operating at around 1150°C.

TCS itself is produced by reacting MG silicon with dry hydrochloric acid in a fluidized bed reactor in the presence of copper as catalyst at moderate temperatures (250°C): the crude product, consisting of about 90% of TCS, is then purified by distillation and exchange resins absorption.

The reduction reaction, formally written as

$$SiHCl_3 + H_2 \leftrightarrow Si + 3HCl \quad (7)$$

occurs with conversion rates which depend on the H_2/TCS ratio and amounts to about 30% in a single-step process. Actually, the reactor outstream contains a mixture of chlorosilanes, whose relative amount depends on the reactor parameters.

To get higher process efficiencies, the recycling of unreacted TCS and the catalytic conversion of chlorosilanes to TCS is systematically carried out in its more modern versions, in which the input product is crude TCS and the output is high-purity poly-silicon. The major drawback of the Siemens C process is its high energy intensity, with a limiting target value less than 120 kWh/kg. This value seems to be hard to be reduced, although the most modern versions of the multibar reactors could provide further improvements.

The final production costs depend on many factors, of which that of the electric energy is one of the most relevant, but a figure around 40–50 €/kg seems to be realistic.

An already working process, alternative to the, Siemens C route and originally developed by Ethil Corp., is operated by MEMC Electronic Materials in Pasadena (USA) [81].

This process is based on the pyrolitic decomposition of monosilane (SiH_4) in a fluidized bed reactor, where the silicon powder provides the sites for the heterogeneous nucleation and further growth to silicon grains.

SiH_4 itself is produced with a proprietary process starting from MG silicon, which is reacted in a fluidized bed with HF at low pressure, and is characterized by a high rejection ratio for metallic and non-metallic impurities except for carbon. Carbon fluoride gaseous compounds and hydrocarbons are converted to methane with the use of a catalyst. SiF_4 is purified in a regenerated absorber with removal of traces of HF and H_2O and condensed in a cryogenic condenser–evaporator under pressure.

SiF_4 is then reacted with calcium hydride in a reactor of proprietary design, where calcium hydride is dissolved in a molten mixture of CaF_2.

In this case the product is an ultra-pure granular poly-silicon, which provides tremendous cost and productivity advantages over traditional "chunk" of poly-silicon in the CZ growth process. According to MEMC Electronic materials the total electric energy consumption is around 19 kWh/kg and the production cost is around 25 $/kg.

Eventually, Deutsche Solar [82–84] announced the introduction into the market of powder silicon produced by decomposition of silane. Here, SiH_4 is produced on the base of a Degussa patent via the disproportionation of TCS produced from MG silicon

$$4SiHCl_3 \leftrightarrow SiH_4 + 3SiCl_4 \quad (8)$$

After several purification steps, pure silane is pyrolized in an open space reactor. The product is a very fine silicon powder which must be mechanically compacted before its use in a casting furnace.

Today also SiH_4 is considered also as a possible reactant in a Siemens type of reactor.

5.2 Solar silicon from MG silicon

Very complex looked [85] and still looks [86–88] the solution of problems associated with the production of solar grade silicon using variants of the metallurgical (MG) silicon process, with the aim to find an alternative route for the production of a low-cost, low-energy intensive poly-crystalline feedstock. In the past it was, in fact, figured that any material based on this process would contain a too large amount of impurities and structural defects. For this reason, the MG silicon route was considered almost impracticable, due to the difficulty of removal of tens of ppmw of boron and phosphorous, hundreds of ppmw of carbon and thousands of ppma of metallic impurities.

More recently, the abrupt increase of the worldwide request of EG-Si feedstocks and the subsequent silicon material shortage, addressed a major interest to the MG silicon route. The objective is to produce *clean* MG silicon by the understanding of the role of impurities and crystal defects on the minority carrier lifetime and minority and majority carrier's mobility and to discover/develop remedies in their presence.

Taking as demonstrated that silicon poly-crystal feedstocks from the *gas-phase* routes will be mostly employed for the Cz growth of single-crystal ingots, and then for the manufacture of thin highly efficient ($\gg$18%) single-crystal solar cells, the solar silicon from the MG route would be the main feedstock for the multi-crystalline silicon route.

This means that here is the problem is two-fold, as there is the need to develop innovative routes for the production of high-quality MG silicon and to improve its properties before or during the solar cell manufacturing process. This requires developing an appropriate gettering and defect passivation

Table 1 Impurity distribution in ppmw along a DS ingot grown from a lightly purified MG silicon (slice number counted from the bottom to top of the solidification front)

Element	Starting concentration (ppmw)	Slice nr						
		19	21	23	50	52	54	Top
Al	52	2.0	3.0	2.0	4.0	2.7	5.5	>1500
B	3.0	2.5	2.1	2.2	2.4	3.1	3.1	8.7
P	6.0	3.2	3.4	6.8	8.8	6.1	11	300
Ca	36	48	67	91	135	>150	>150	>1500
Mg	14	19	27	40	62	70	60	250
Fe	33	3.4	<1	<1	1.7	<1	2.0	>6000
Ti	32	<1	<1	<1	<1	<1	1,7	>1500

Table 2 Effective segregation coefficients of metallic impurities in DS grown multi-crystalline silicon ingots from purified MG feedstocks in comparison to CZ silicon

Element	Effective Cz	Effective DS
Cu	6.9×10^{-4}	2×10^{-3}
Cr	1.1×10^{-5}	3.7×10^{-3}
Fe	6.4×10^{-6}	1.6×10^{-4}
Ni	3.2×10^{-5}	9×10^{-4}
Ti	3.6×10^{-6}	2.5×10^{-3}
Zr	1.5×10^{-8}	7.7×10^{-4}

techniques, in the presence of extended defects, which could behave as deep sinks for residual impurities and then compete with external sinks.

5.3 Towards the use of solar grade silicon

This kind of material should be obtained by the development of a new technology either based on appropriate refining processes of commercial MG silicon or on a new/improved MG silicon production process.

The results of systematic studies carried out in the last twenty years showed already where the problems are that should be overcome to succeed in the industrialisation of solar silicon production via the MG route.

As an example, our past studies [89] about the segregation profile of impurities in DS ingots grown from a pre-purified MG silicon feedstock showed (see as example Table 1) that most of the impurities collect on the very top of the ingot. As forecasted, metallic impurities behave better than alkali earth impurities, while B and P could not be removed, although the behaviour of P is better than that of B.

It is quite apparent that this material is very far from solar grade quality and remains this way even after two DS crystallizations, as B and P could not be brought to the proper level. Therefore, a preliminary refining step should be carried out should before the final directional solidification, in order to remove B and P and to decrease the concentration of the other impurities. It was also demonstrated (see Table 2) that the effective segregation coefficients of impurities in a DS growth deviate systematically from those experimented in the conventional crucible CZ growth.

The differences are particularly large in the case of Ti and Zr, important in the case of iron, but they are still sufficiently small to get in any case a significant purification of a silicon feedstock of MG origin.

These last results show also that the thermodynamics of impurity segregation during the liquid/solid equilibrium is influenced by the presence of extended defects (GBs and dislocations) at the solid branch of the (moving) interface where the growth occurs epitaxially. Extended defects behave apparently as heterogeneous nucleation centres for supersaturated impurities as well as gettering sites. The strong deviations relative to Zr and Ti, both very reactive with oxygen, indicate also a possible influence of dissolved oxygen on their effective segregation coefficient, in good agreement with previous considerations about the interaction of oxygen with extended defects.

A penalty to be paid, therefore, when mc-solar grade silicon is used as a solar cell substrate, is associated with the simultaneous presence of impurity contaminated grain boundaries and dislocations, which invariably will worsen the conversion efficiency of solar cells fabricated with this material, unless these materials are submitted to appropriate gettering procedures [69].

5.4 Solar grade silicon purification procedures

The main stream for the production of solar grade silicon consists in a series of processes aimed at the selective removal of different impurities from commercial metallurgical grade silicon. Generally, the first step is a treatment of

liquid silicon, directly poured in a ladle from the carbothermic furnace, with suitable gases or slags for the (partial) removal of B and P. The second step consists in the acid leaching of the material obtained in the first step, after crushing and milling to fine powder. This step is addressed at the removal of metallic impurities. The final step is the directional solidification of the material obtained with the leaching treatment, after melting in a conventional growth furnace.

Boron and phosphorous removal We have seen in the previous section that directional solidification is unable to remove B and P from a highly doped ingot, due to the values of the segregation coefficients which are close to one.

The problem of B removal was tackled, among others, by Khattak and co-workers [90, 91], which showed that wet argon bubbling is very effective in B removal. In fact, it was demonstrated that the B could reduced to 0.3 ppma from original levels of 40–60 ppma. The experiments were carried out in a heat exchanger method (HEM) furnace, with silicon charges up to 300 kg. The chemistry of this process is based on the formation of volatile HBOx species, which escape from the reaction phase and give rise to a condensate on the cold walls of the reactor. With these procedures, also the P content is reduced to less than 7 ppma from an average content of 45 ppma. However, the final P content is still too high for PV applications, and it should be removed in a second process step, based on a liquid–liquid extraction technique.

Liquid–liquid extraction with basic slags are, in fact, very effective in P removal [92] as was also demonstrated by Pizzini and co-workers [93], who showed that this technique works satisfactorily also with B.

Liquid–liquid extraction techniques with acid slags under oxidizing conditions are also effective in removing alkali earth impurities (Ca, Sr, Ba and Mg) and Al [92]. Here the simultaneous bubbling of oxygen is necessary in order to oxidize metals to oxides, which then dissolve in the molten silicate/carbonate slags.

Liquid–liquid extraction techniques based on the use of oxynitride slags, which are shown to work as sinks for B and P, were also proposed [94].

All these processes must be, however, applied, under any industrial application conditions, on charges of several hundreds of Kg, in suitable ladles where the silicon charge should be maintained liquid for the time requested for its purification without unwanted impurity contamination arising from the internal lining of the process ladle.

In the work of Khattak previously cited [92] it was also shown that only pure quartz crucibles work in the proper conditions, as any other kind of refractory container or liner causes severe contamination problems.

An alternative approach for P removal from highly P-doped feedstocks or from MG silicon could be based on selective P evaporation procedures, considering that the P partial pressure in P-doped silicon at the melting temperature of silicon is well-known to be much lower than that of Si. However, P-evaporation under vacuum suffers of problems associated to the removal of condensed P at the reactor walls and extensive Si losses, which, to the author's experience, might limit the applicability of this process to industrial applications, without radical changes in the conduction of the evaporation process.

More recently, the problem was tackled starting from the solution of Si or quartz in suitable acids and to conduct the B and P removal directly in solution [95]. Another way to do it might be via the use of plasma torch techniques, as done by Amouroux et al. [96, 97]. In this case, the addition of minute amounts (0.1%) of oxygen to the process argon plasma enhances the removal of B from MG-Si due to the formation of volatile boron oxides.

The process developed by Kawasaki Steel [98, 99] consists instead of a first stage where P is removed under vacuum and of a second stage where B is removed using a non transfer arc wet argon plasma. Solar cells manufactured with this material showed conversion efficiency of the order of 12%.

Today, therefore, the B and P removal from highly doped silicon remains a problem which has not yet found a definitive solution, in spite of recent Timminco claims [100].

Metallic impurities removal Most of the metallic impurities might be removed by DS processes, but their concentration could be reduced by one single DS step to solar quality provided their initial concentration ranges around few ppma, as the average values of the segregation coefficients are around 10^{-3}. In the case of commercial MG Si their average content is much greater than 100 ppma, and, therefore their content should be reduced of a factor at least 100 or more by different methodologies before DS solidification. The process adopted since the early 1980s at the Wicker [101] and Heliosil Laboratories was based on the acid leaching of MG-Si powder, obtained by grinding the silicon metal to a 20 µm powder, possibly after a preliminary liquid–liquid extraction step addressed at B and P removal [92]. As it is well-known from thermodynamics, the surface composition of a multicomponent phase is different from that of the bulk, and impurities therefore might segregate at the surface if there is a net energy advantage. We have already tackled this problem while considering the effect of grain boundaries showing that the chemical potential of an impurity at a surface is different from that in the bulk as a consequence of different coordination and, possibly, of a different oxidation state [102].

Leaching therefore must succeed in a selective removal of the slag phase and of the metals segregated at the surface

of the silicon grains. This procedure, as it is well-known, is based on the fact that silicon is un-soluble in HCl and only slightly soluble in HF alone, leaving to these acids the potential of dissolving only a second non-metallic phase, if present, and of the impurities segregated at the surface.

This process suffers, however, of several drawbacks, as the fine silicon powder is pyrophoric and hydrogen evolves during the acid leaching of silicon, possibly causing explosive consequences. Moreover, melting a fine silicon powder is a very difficult task as it is known from recent literature concerning, as an example, the Deutsche Solar Process [82, 83] (see Sect. 5.1).

5.5 The Elkem process

The Elkem process today is already close to the industrialization and consists essentially in a preliminary boron removal step from MG silicon via a liquid–liquid extraction procedure, using an alkali metal silicate as the extractant. Then silicon is crushed to a fine powder and metallic impurities are removed by acid leaching. Eventually, the material is melted in a DS furnace, where the final purification is carried out [103, 104].

Solar cells manufactured from this material showed efficiency greater than 15%.

The approach used follows practices already set-up in the 1980s, as shown in the former Sections, and presents the advantage to start from a very cheap material, produced with a much known technology worldwide in million ton amounts.

6 Conclusions

Reduction in silicon wafer thickness and kerf loss in wafering procedures will certainly lower the silicon feedstock consumption problems in the years to come giving EG polycrystalline silicon the major chance to sustain the annual PV growth [105] considering the today's forecasts that it will be available in more than in amounts of 60,000 tons/year after the year 2010.

It is, however, easy to forecast that severe environmental problems, mostly associated to the use of silicon halides and the high energy costs, will limit the expansion of the gas-phase processes leaving the best opportunities to solar silicon of metallurgical (MG) origin. As it has been shown here, this is still a chance and a challenge but not an impossible target.

Acknowledgements The author is strongly indebted to M. Acciarri and S. Binetti for suggestions and criticisms during the preparation of this paper and for years of close activities in the field of silicon-based materials.

References

1. Materials Today, Vol. 9, June 2006; Materials Today, vol. 10, November 2007
2. http://www.eupvplatform.org
3. J.R. Davis, R.H. Hopkins, A. Rothagi, in *Materials and New Processing Technologies for Photovoltaics*, ed. by J. Dismukes, E. Sirtl, P. Rai-Chaudhury, L.P. Hunt. Proc. vol. 82(8) (Electrochem. Soc., New York, 1982), p. 14
4. R.H. Hopkins, J.R. Davis, A. Rothagi, M.H. Hanes, P. Rai-Chaudhury, Final Report, Contract 954331 JPL 9950 (1982)
5. S. Pizzini, in *Silicon Processing for Photovoltaics I*, ed. by C.P. Chattak, K.V. Ravi (Elsevier, Amsterdam, 1985), pp. 169–206
6. J. Brody, A. Rohatgi, V. Yelendur, Prog. Photovolt. Res. Appl. **9**, 273 (2001)
7. N.B. Mason, T.M. Bruton, S. Gledhill, K.C. Heasman, O. Hartley, C. Morilla, S. Roberts, in *Proc. 19th European Photovoltaic Solar Energy Conference* (2005), p. 1198
8. H. Helmreich, in *Silicon Processing for Photovoltaics II*, ed. by C.P. Khattak, K.V. Ravi (Elsevier, Amsterdam, 1987), p. 97
9. S. Pizzini, M. Gasparini, M. Rustioni, Certificat d'utilitè 82 12588, July 1982
10. N. Stoddard, B. Wu, I. Witting, M. Wagener, Y. Park, G. Rozgonyi, R. Clark, Solid State Phenom. **131–133**, 1–8 (2008)
11. J. Foggiato, W.S. Yoo, M. Ouaknine, T. Murakami, T. Fukada, Mater. Sci. Eng. B **114–115**, 56 (2004)
12. J. Lu, M. Wagener, G. Rozgonyi, J. Rand, R. Jonczik, J. Appl. Phys. **94**, 140 (2003)
13. S. Binetti, M. Acciarri, C. Savigni, A. Brianza, S. Pizzini, A. Musinu, Mater. Sci. Eng. B **36**, 68 (1996)
14. A.A. Istratov, H. Hieslmair, E.R. Weber, Appl. Phys. A **70**, 489 (2000)
15. S. Martinuzzi, S. Pizzini, in *Advanced Silicon and Semiconducting Silicon-based Alloy Based Materials and Devices*, ed. by J.F. Nijs (Institute of Physics Publ., 1994), Chap. 9, pp. 323–357
16. L.Q. Nam, M. Rodot, M. Ghannam, J. Coppye, P. De Schepper, J. Nijs, D. Sarti, I. Perichaud, S. Martinuzzi, Int. J. Solar Energy **11**, 273 (1992)
17. S. Pizzini, P. Cagnoni, A. Sandrinelli, M. Anderle, R. Canteri, Appl. Phys. Lett. **51**, 676 (1987)
18. W.K. Tice, T.Y. Tan, in *Defects in Semiconductors*, ed. by J. Narayan, T.Y. Tan (North Holland, Amsterdam, 1981), p. 367
19. S.M. Hu, in *Oxygen, Carbon, Hydrogen and Nitrogen in Crystalline Silicon*. MRS Proc., vol. 59 (1987), p. 249
20. J.M. Hwang, D.K. Schroeder, J. Appl. Phys. **59**, 2476 (1986)
21. S. Pizzini, Phys. Stat. Sol. A **171**, 123 (1999)
22. V. Kveder, M. Badylevich, E. Steinman, A. Izotov, M. Seibt, W. Schroeter, Appl. Phys. Lett. **84**, 2106 (2004)
23. W. Seifert, G. Morgenstern, M. Kittler, Semicond. Sci. Technol. **8**, 1687 (1993)
24. J. Chen, T. Sekiguchi, D. Yang, F. Yin, K. Kido, S. Tsurekawa, J. Appl. Phys. **96**, 5490 (2004)
25. J. Chen, T. Sekiguchi, S. Ito, D. Yang, Solid State Phenom. **131–133**, 9–14 (2008)
26. J. Chen, T. Sekiguchi, S. Nara, D. Yang, J. Phys. Condens. Matter. **16**, S211 (2004)
27. J. Chen, D. Yang, Z. Xi, T. Sekiguchi, J. Appl. Phys. **97**, 033701 (2005)
28. C.R.M. Grovenor, J. Phys. C **18**, 4079 (1985)
29. K. Yang, G.H. Schwuttke, T.F. Ciszek, J. Cryst. Growth **50**, 301 (1980)
30. H.F. Mataré, J. Appl. Phys. **56**, 265 (1984)
31. A.A.S. Al-Omar, M.Y. Ghannam, J. Appl. Phys. **79**, 2103 (1996)
32. S. Pizzini, M. Acciarri, Mater. Res. Soc. Symp. Proc. **182**, 185 (1990)

33. M. Beghi, C. Chemelli, S. Fossati, S. Pizzini, in *Poly-micro Cristalline and Amorphous Semiconductors*, ed. by P. Pinard, S. Kalbitzer (Les Editions de Physique, Les Ulis, 1984), p. 181
34. B.L. Sopori, L. Jastrzebski, T. Tan, S. Narayan, in *Proceedings of the 12th European Photovoltaic Solar Energy Conference*, The Netherlands (1994), p. 1003
35. S.A. McHugo, H. Hieslmair, E.R. Weber, Appl. Phys. A **64**, 127 (1997)
36. S. Pizzini, A. Sandrinelli, M. Beghi, D. Narducci, F. Allegretti, S. Torchio, G. Fabbri, G.P. Ottaviani, F. Demartin, A. Fusi, J. Electrochem. Soc. **135**, 157 (1988)
37. Z.J. Radzimski, T.Q. Zhou, A. Buczkowski, G.A. Rozgonyi, D. Finn, L.G. Hellwig, J.A. Ross, Appl. Phys. Lett. **60**, 1096 (1992)
38. M. Kittler, W. Seifert, O. Krüger, Solid State Phenom. **78–79**, 39 (2001)
39. B. Shen, T. Sekiguchi, J. Jablonski, K. Sumino, J. Appl. Phys. **76**, 4540 (1994)
40. W. Shockley, W.T. Read, Phys. Rev. **87**, 835 (1952)
41. L. Pelosini, A. Parisi, S. Pizzini, U.S. Patent 4,241,037, 23 Dec 1980
42. C.P. Khattak, D.B. Joyce, F. Schmid, Final Report NREL/SR-520-30716
43. S. Pizzini, C. Calligarich, J. Electrochem. Soc. **131**, 2128 (1984)
44. L.J. Gerligs, D. McDonnals, G. Coletti, in *17th NREL Workshop on Crystalline Solar Silicon Cells & Modules: Materials and Processes*, Vail, Colorado (2007), p. 169
45. T. Tatsumi, H. Hirayama, N. Aizaki, Jpn. J. Appl. Phys. **27**, L954 (1988)
46. E. De Fresart, K.L. Wang, S.S. Rhee, Appl. Phys. Lett. **53**, 48 (1988)
47. S. Pizzini, F. Borsani, A. Sandrinelli, D. Narducci, F. Allegretti, in *Point and Extended Defects in Semiconductors* (Plenum, New York, 1989), p. 105
48. M. Rodot, J.E. Bourèe, A. Mesli, G. Revel, R. Kishore, S. Pizzini, J. Appl. Phys. **62**, 2556 (1987)
49. S. Martinuzzi, M. Zehaf, H. Poitevin, G. Mathian, M. Pasquinelli, in *Proc. 18th Photovoltaic Specialist Conference*, Las Vegas (IEEE Press, New York, 1985), p. 1127
50. R.L. Marchand, C.T. Sah, J. Appl. Phys. **48**, 336 (1977)
51. S. Borghesi, M. Geddo, G. Guizzetti, S. Pizzini, D. Narducci, A. Sandrinelli, G. Zachmann, Solid State Commun. **69**, 457 (1989)
52. S. Pizzini, M. Acciarri, C. Savigni, A. Brianza, S. Pizzini, A. Musinu, Mater. Sci. Eng. B **36**, 68 (1996)
53. S. Pizzini, M. Acciarri, S. Binetti, Solid State Phenom. **19–20**, 479 (1991)
54. S. Pizzini, M. Acciarri, S. Binetti, in *Defects in Silicon*. Electrochemical Soc. Proc. (1991), p. 155
55. S. Pizzini, F. Borsani, M. Acciarri, Mater. Sci. Eng. B **4**, 353 (1989)
56. S. Pizzini, E. Leoni, S. Binetti, M. Acciarri, A. LeDonne, B. Pichaud, Solid State Phenom. **95–96**, 273 (2003)
57. C. Beluet, in *Silicon Processing for Photovoltaics I*, ed. by C.P. Chattak, K.V. Ravi (Elsevier, Amsterdam, 1985), pp. 87–129
58. S. Pizzini, C. Calligarich, C. Chemelli, M. Gasparini, P. Rava, L. Sardi, in *Materials and New Processing Technologies for Photovoltaics*, ed. by J.A. Amick, J. Dietl, V.K. Kapur. Proc. vol. 83(11) (Electrochemical Soc., New York, 1983), p. 200
59. S. Pizzini, L. Bigoni, M. Beghi, C. Chemelli, S. Fossati, M. Tincani, J. Electrochem. Soc. **133**, 2363 (1986)
60. A.A. Istratov, T. Buonassisi, M.D. Pickett, M. Heuer, E.R. Weber, Mater. Sci. Eng. B **134**, 282 (2006)
61. D. MacDonald, J. Tan, R. Bardos, Th. Trupke, in *Proc. 22nd European Photovoltaic Solar Energy Conference*, Milan, Italy, pp. 820–828
62. A.A. Istratov, T. Buonassisi, R.J. McDonald, A.R. Schmidt, R. Schindler, J.A. Rand, J.P. Kalejs, E.R. Weber, J. Appl. Phys. **94**, 6552 (2003)
63. D. Macdonald, A. Cuevas, A. Kinomura, Y. Nakano, L.J. Gerligs, J. Appl. Phys. **97**, 33523 (2005)
64. L.J. Gerligs, P. Manshanden, G.P. Wyers, E.J. Overlid, O.S. Raaness, A.N. Waernes, B. Wiersma, in *Proceed. 20nd European Photovoltaic Solar Energy Conference*, Barcelona, Spain, 6–10 June 2005, p. 619
65. D. McDonald, J. Tan, R. Bardos, T. Trupke, in *Proceed. 22nd European Photovoltaic Solar Energy Conference*, Milan, Italy, 3–7 September, p. 820
66. S. Pizzini, in *Defect Interaction and Clustering in Semiconductors*, ed. by S. Pizzini (Scitec Publications, Zuerich, 2002), pp. 1–65
67. V. Kveder, M. Kittler, W. Schröter, Phys. Rev. B **63**(8), 115208 (2001)
68. S.M. Myers, M. Seibt, W. Schröter, J. Appl. Phys. **88**, 3795 (2000)
69. V. Kveder, W. Schröter, A. Sattler, M. Seibt, Mater. Sci. Eng. B **71**, 175 (1999)
70. L.L. Kasmerski, P.G. Ireland, F.T. Ciszek, Appl. Phys. Lett. **36**, 323 (1980)
71. L.L. Kasmerski, P.E. Russel, J. Phys. (Paris) Coll. C **1**(10 Suppl.), 172 (1982)
72. J. Maurice, C. Coliex, Appl. Phys. Lett. **55**, 2 (1989)
73. A. Ihlal, R. Risk, O. Duparc, J. Appl. Phys. **80**, 2665 (1996)
74. S. McHugo, A.C. Thomson, I. Perichaud, S. Martinuzzi, Appl. Phys. Lett. **72**, 3482 (1998)
75. S. McHugo, A.C. Thomson, A. Mohammed, G. Lamble, I. Perichaud, S. Martinuzzi, M. Werner, M. Rinio, W. Koch, H.U. Hoefs, C. Haessler, J. Appl. Phys. **89**, 4282 (2001)
76. T. Buonassisi, M.A. Marcus, A. Istratov, M. Heuer, T.F. Ciszek, B. Lai, Z. Cai, E.R. Weber, J. Appl. Phys. **97**, 063503 (2005)
77. M.V. Trushin, O.F. Vyvenko, M. Seibt, Solid State Phenom. **131–133**, 155–160 (2008)
78. S. Pizzini, M. Donghi, S. Binetti, G. Wagner, M. Bersani, J. Electrochem. Soc. **145**, Ll8 (1998)
79. S. McHugo, Appl. Phys. Lett. **71**, 1984 (1997)
80. V. Kveder, M. Badylevich, E. Steinman, M. Seibt, W. Schroeter, Appl. Phys. Lett. **64**, 2106 (2004)
81. MEMC web page
82. R. Sonnenschein, A. Müller, T. Sill, A. Golz, P. Adler, in *Silicon for the Chemical Industry VIII*, Trondheim, Norway, 12–16 June 2006
83. A. Müller, R. Sonnenschein, T. Sill, A. Golz, P. Adler, in *Proc. 20th European Photovoltaic Solar Energy Conference*, Barcelona, Spain, pp. 623–626
84. PRESS Release 26.06.2006 (Deutsche Solar)
85. S. Pizzini, Sol. Energy Mater. **6**, 253 (1982)
86. K. Morita, T. Miki, Intermetallics **11**, 1111 (2003)
87. A.A. Istratov, T. Buonassisi, M.D. Pickett, M. Heuer, E.R. Weber, Mater. Sci. Eng. B **134**, 282 (2006)
88. J.L. Gerlichs, B. Ceccaroli, O. Lohne, in *Handbook of Photovoltaic Science and Engineering*, ed. by A. Luque, S. Hegedus (Wiley, New York, 2003), Chap. 5
89. S. Pizzini, M. Rustioni, Unpublished results
90. C.P. Khattak, D.B. Joyce, F. Schmid, Sol. Energy Mater. Sol. Cells **74**, 77 (2002)
91. C.P. Khattak, D.B. Joyce, F. Schmid, Final Report NREL/SR-520-30716
92. C.P. Khattak, D.B. Joyce, F. Schmid, in *Proc. 29th Photovoltaic Specialist Conference* (IEEE Press, New York, 2004)
93. L. Pelosini, A. Parisi, S. Pizzini, U.S. Patent 4,241,037, 23 Dec 1980
94. D.C. Lynch, H.A. Oye, U.S. Patent 2007/0245854 A1

95. S. Amendola, International Patent C01B 33/00 (2006.01) WO 2007/106860
96. J. Amouroux, D. Morvan, U.S. Patent 4399116-28/07/1981
97. D. Morvan, J. Cazard-Avernat, J. Amouroux, Rev. Phys. Appl. **18**, 239–251 (1983)
98. K. Hanazawa, M. Abe, H. Baba, N. Nakamura, B. Yuge, Y. Sakaguchi, Y. Kato, S. Hiwasa, M. Obashi, in *Proceed. PVSEC-12*, Jeju, Korea, pp. 265–268
99. Y. Kato, Y. Sakaguchi, S. Hiwasa, Prog. Photovolt. Res. Appl. **9**, 203–209 (2001)
100. Photon International, 6/2008, pp. 108–109
101. J. Dietl, in *Proc. Eigth European Photovoltaic Solar Energy Conference*, pp. 599–605
102. S. Pizzini, in *Defects in Electronic Ceramics, Material Sci. Forum*, vol. 116 (1993), pp. 81–120
103. K. Peter, E. Enebakk, K. Friestad, R. Tronstad, C. Dethloff, in *Proc. 20th European Photovoltaic Solar Energy Conference*, Barcelona, Spain, 6–11 June 2005, p. 615
104. J. Vedde, R. Tronstad, in *Proc. 21th European Photovoltaic Solar Energy Conference*, Dresden, Germany, 2006
105. N.B. Mason, in *Proc. PV Science, Applications& Technology Conf.*, Durham UK, 28–30 March 2007, p. 41